Dynamic Modeling of a Three-Way Catalyst for SI Engine Exhaust Emission Control

E. P. Brandt, Yanying Wang, and J. W. Grizzle

Abstract— **Automotive emissions are severely regulated. Since 1980, a three-way catalyst (TWC) has been used to convert harmful emissions of hydrocarbons, carbon monoxide, and oxides of nitrogen into less harmful gases in order to meet these regulations. The TWC's efficiency of conversion of these gases is primarily dependent on the mass ratio of air to fuel (A/F) in the mixture leaving the exhaust manifold and entering the catalyst, the velocity of the exhaust mass, and the temperature of the catalyst. The goal of this paper is to develop a dynamic, control-oriented model of a TWC. First, the measurement capabilities will be described. Then, a simplified, dynamic catalyst model that can be determined on the basis of medium bandwidth A/F measurements and low bandwidth temperature and emission measurements will be developed and validated.**

Keywords— **Control systems, modeling, nonlinear systems, road vehicles.**

I. INTRODUCTION

A. Problem statement and motivation

California and Federal emissions regulations for 2000 and beyond, in combination with customer performance demands, are engendering significant mechanical design changes to the basic internal combustion engine. Examples of innovations include variable displacement engines (VDE), variable cam timing (VCT) engines, and camless engines. These new mechanical features are resulting in a high degree of dynamic coupling, and to be operated effectively, require sophisticated multivariable control systems [1]. The proper design of these controllers requires good fidelity dynamic models of the engine as well as the three-way catalyst (TWC) used to post-treat the engine's exhaust, or feedgas. The three major, EPA-regulated automotive pollutants are carbon monoxide (CO), unburned hydrocarbons (HC), and oxides of nitrogen (NO_x). The TWC is used to convert HC, CO, and NO_x into less harmful components.

The goal of this paper is to develop a simplified model of the TWC that is appropriate for use in controller design for spark ignition engines. Detailed chemical and thermodynamic-based mathematical models of TWC's

E. P. Brandt is with the Electrical Engineering and Computer Science Department, University of Michigan, Ann Arbor, MI 48109-2122, USA, and Ford Motor Company, Ford Research Laboratory, Powertrain Control Systems Department, MD 2036 SRL, P.O. Box 2053, Dearborn, MI 48121-2053, USA. E-mail: brandt@eecs.umich.edu .

Yanying Wang is with Ford Motor Company, Ford Research Laboratory, Powertrain Control Systems Department, MD 2036 SRL, P.O. Box 2053, Dearborn, MI 48121-2053, USA. E-mail: ywang1@ford.com .

J. W. Grizzle is with the Electrical Engineering and Computer Science Department, University of Michigan, Ann Arbor, MI 48109-2122, USA. E-mail: grizzle@eecs.umich.edu .

have been proposed in the literature [2], [3]. While these models seem to be useful for catalyst design, they do not seem suitable for use by a control engineer. Indeed, one problem with these models in an industrial setting is that by the time one is able to determine the values of the various physical parameters in the model for a given catalyst composition, technology advancements will have already driven a change in the TWC's formulation. In addition, the models are typically given by several coupled nonlinear partial differential equations, so working with them for control design is unwieldy.

This work will pursue a phenomenological model of the TWC that can be tuned quite rapidly to data. The model's formulation will be centered around the mass ratio of air to fuel (air-fuel ratio, or A/F), since this a fundamental variable in most engine models [2], [3], [4], [5], [6], [7] and there exist standard sensors for on-board A/F measurement.

In addition to its utility in controller design, a dynamic catalyst model may be useful in the development of improved diagnostic algorithms. The OBD-II standard (second phase of EPA on-board diagnostic regulations for automobiles) requires manufacturers to monitor catalyst performance and light the *Check Engine* light if tailpipe emission levels remain above 1.5 times the standard for a specified period of time. This is increasingly difficult as newer emission standards require lower and lower levels of exhaust gases at the tailpipe. To meet this requirement for ULEV (ultra-low emission vehicle), this diagnostic will have to determine the difference between a catalyst that is working at 96% efficiency (which is good) and 94% efficiency (which is bad).

B. Outline of paper

Section II provides background information on the three-way catalyst and motivation for the modeling strategy that is pursued. Section III describes the testing facilities available for the work done in this paper. The model development is described in Section IV, and the model's performance is evaluated in Section V. Section VI concludes with a summary and highlights some remaining issues.

II. BACKGROUND
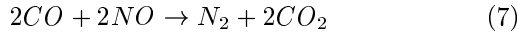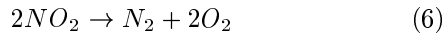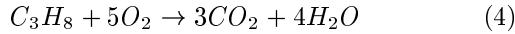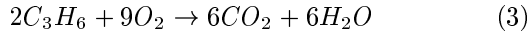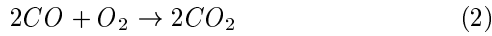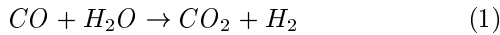
A. Basics of the TWC and emissions testing

Catalytic converters were first used to post-treat exhaust feedgas in production automobiles beginning in 1975 in order to meet emission control regulations [8]. These catalysts were oxidation catalysts, also known as two-way catalysts, since they oxidized HC and CO, converting them to CO_2 and water vapor (H_2O). In 1980, the catalytic

converter was enhanced with the ability to reduce NO_x as well [9], giving rise to the so-called three-way converter. The primary chemical reactions that take place in a warm, properly functioning TWC are as follows [3]:

$$CO + H_2O \rightarrow CO_2 + H_2 \tag{1}$$
$$2CO + O_2 \rightarrow 2CO_2 \tag{2}$$
$$2C_3H_6 + 9O_2 \rightarrow 6CO_2 + 6H_2O \tag{3}$$
$$C_3H_8 + 5O_2 \rightarrow 3CO_2 + 4H_2O \tag{4}$$
$$2H_2 + O_2 \rightarrow 2H_2O \tag{5}$$
$$2NO_2 \rightarrow N_2 + 2O_2 \tag{6}$$
$$2CO + 2NO \rightarrow N_2 + 2CO_2 \tag{7}$$

A catalytic converter does not work efficiently until it reaches a sufficiently high temperature, in the range of 650°F. When a catalyst is cold, neither the reduction of NO_x nor the oxidation of CO or HC occur within the converter. As the catalyst warms up, these reactions occur more completely. The catalyst is commonly said to *light off* when HC conversion efficiency reaches 50%.

Typical modern catalysts are of the monolithic type, as pictured in Fig. 1. In this type of converter, the exhaust gas passes through a honeycomb ceramic block, maximizing the exposed surface area. The ceramic block is covered with a thin coating of platinum, palladium, or rhodium, and mounted in a stainless steel container.
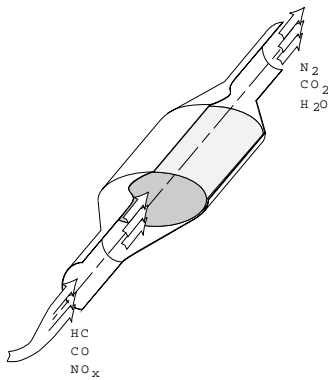

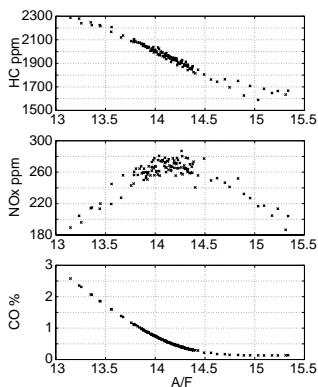Fig. 1. Monolithic-type catalytic converter
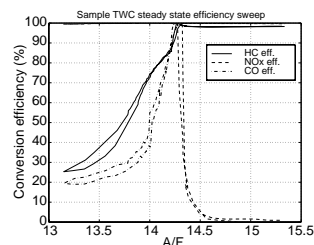

Fig. 2. Feedgas emissions vs. A/F

Fig. 3. Sample steady state TWC efficiency data (forward and backward sweeps).

Figures 2 and 3 show representative emissions data collected under steady state conditions. These curves only apply to *static A/F* conditions. However, typical engine operation is dynamic, and as will be discussed in Section III, measuring instantaneous emissions is very difficult. In order to determine whether or not a vehicle meets emissions requirements, the EPA has specified a test which totally obviates this issue. The vehicle under-test is placed on a chassis dynamometer and driven through a specific (dynamic) drive cycle which includes neutral and drive idle, accelerations and decelerations of various rates, and cruises. This is known as the Federal Test Procedure (FTP cycle), or *bag test*, since the tailpipe emissions are literally collected into bags. The first 505 seconds of the test are begun when the engine is cold (70°F) and is called Bag 1. The test continues for another 867 seconds, at which point the vehicle is shut off. This completes Bag 2. After a 10-minute soak, the 505-second Bag 1 test is repeated with the warm engine. This part of the test is called Bag 3. The mass of each emission component is then measured and divided by the length of the test in miles to obtain the grams per mile measurement. The overall measurement incorporates emissions accumulated during Bags 1-3. For the sake of completeness, the vehicle speed profile for Bags 1 and 2 is shown as Fig. 4.
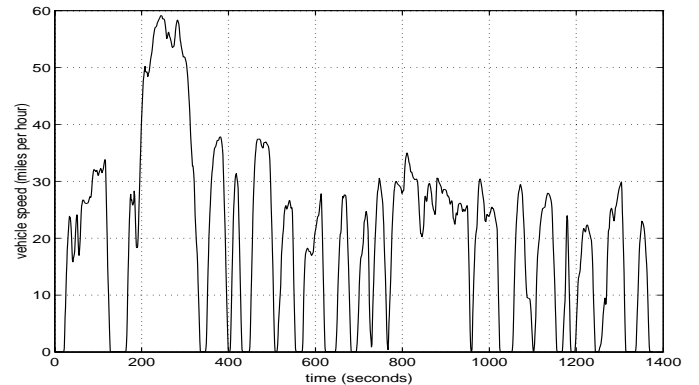

Fig. 4. FTP cycle trace.

| | Emissions standards (grams per mile) | | | | | |
| | HC | | CO | | NO_x | |
	50K	100K	50K	100K	50K	100K
pre-CAA	0.390	NONE	7.0	NONE	0.4	NONE
CAA	0.250	0.310	3.4	4.2	0.4	0.6
TLEV	0.125	0.156	3.4	4.2	0.4	0.6
LEV	0.075	0.090	3.4	4.2	0.2	0.3
ULEV	0.040	0.055	1.7	2.1	0.2	0.3

TABLE I

PROGRESSION OF REGULATORY STANDARDS FOR VEHICLE EMISSIONS IN CALIFORNIA.

B. Key phenomenon: oxygen storage

The dynamics of a TWC include a phenomenon called *oxygen storage*. When NO_x is reduced, as in (6), oxygen (O_2) is left as a by-product of the reaction, and O_2 is

consumed when HC and CO are oxidized, as in (2)–(4). However, if more O_2 is released than is used, the remaining oxygen will be stored (up to a certain capacity) in the catalyst. Conversely, if more O_2 is used than released, the catalyst will give up oxygen (as long as some is available) to the reduction reaction to allow it to happen. There are two primary mechanisms by which oxygen is chemically stored, and the chemical reactions for each of these are shown below:

$$4CeO_2 \rightleftarrows 2Ce_2O_3 + O_2 \qquad (8)$$
$$2PdO \rightleftarrows 2Pd + O_2 \qquad (9)$$
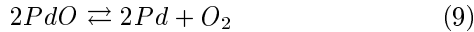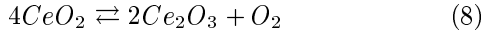
Equation (8) is the primary oxygen storage mechanism that is built into TWC's [3], while the mechanism of (9) is a favorable consequence of the inclusion of palladium in the catalytic material.

The dynamic modeling effort will center on capturing the oxygen storage phenomenon, similarly to the work in [10]. The extent of this phenomenon can be appreciated from Figs. 5 and 6, which depict the A/F response to a step across stoichiometry. Specifically, the steps are taken from 0.5 A/F rich to lean and vice versa at 2000 rpm and 55 ft-lb of torque. The plateau that occurs near the stoichiometric A/F point when transitioning across it in either direction is a manifestation of oxygen storage. Note also that the time that it takes for *breakthrough* (significant departure in equivalent tailpipe A/F[1] from stoichiometry) depends on the direction of the transition.
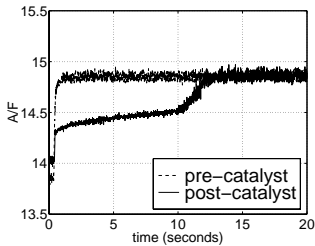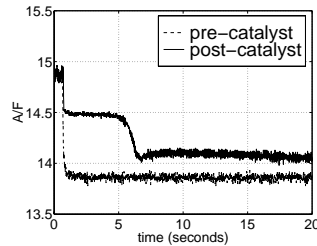

Fig. 5.   Rich-to-lean A/F step

Fig. 6.   Lean-to-rich A/F step

The oxygen storage capacity depends on the flow rate. At low flow rates (50 lb/hr, engine idle), the TWC takes approximately twice as long to break through as it does at high flow rates. The breakthrough time steadily decreases until a mass air flow (MAF) rate of 80 lb/hr is reached. However, the breakthrough time at 80 lb/hr remains constant through higher flow conditions. This was demonstrated in the dynamometer test cell by running the engine at various MAF rates, as high as 240 lb/hr (3000 rpm and 60 ft-lb of torque). All of these higher flow rates showed the same breakthrough time as was seen at 80 lb/hr.

---

[1] The A/F of the exhaust feedgas is a well-defined quantity since mass is conserved during the combustion process. The notion of the "A/F" of the tailpipe exhaust is less clear because mass is not instantaneously conserved through the TWC; indeed, oxygen is stored and released in the catalyst. By A/F for a given volume of exhaust gas at the tailpipe is meant the mass ratio of oxygen to hydrogen and carbon, whether free or combined, respectively, divided by 0.21. When applied to the feedgas, this yields the usual number. If the fuel is oxygenated (reformulated gasoline), a one- to two-percent correction to this would need to be added.

III. EXPERIMENTAL SETUP

A. General

A production platinum-palladium-rhodium TWC was installed on the right bank of a 3.0L-4V engine in a dynamometer test cell. Two types of tests were performed on the catalyst: A/F sweeps and modulation. The A/F sweeps were controlled by software written in LabVIEW. The data acquisition computer used a National Instruments MIO-64-E3 board which allows 64 analog input channels with 12 bit resolution.

Air-fuel ratio is varied by adjusting the fuel injector pulse widths via LabVIEW. A 360-pulses-per-revolution optical encoder was mounted to the crankshaft of the engine. When a pulse width was requested, a calculation was performed to determine the crank angle at which the fuel injection should begin in order to have the desired pulse width end just prior to the opening of the intake valve. The pulse width of each injector was trimmed at stoichiometry to effectively balance the A/F ratio on a cylinder-to-cylinder basis. The engine throttle was controlled by a stepper motor connected directly to the throttle plate. During A/F sweeps and transient tests, the throttle was held constant, maintaing roughly constant mass air flow (MAF). All adjustments to the A/F were made by adjusting the fuel injector pulse width. Mass air flow is measured by a production MAF sensor. The TWC brick temperature is measured with a thermocouple placed one inch into the catalytic material, and the thermocouple used to measure inlet gas temperature is positioned in the exhaust pipe just before the TWC.

B. Emission measurements and caveats

Pre- and post-catalyst emissions were simultaneously measured by two Pierburg AMA-2000 exhaust emission benches. These are comprised of several separate exhaust analyzers, and include a Flame Ionization Detector (FID) for total hydrocarbons and a Chemiluminescence Detector (CLD) for NO_x, both made by Pierburg. The benches also include Rosemount low CO, high CO, and CO_2 analyzers, based on infrared absorption.

For the purposes of dynamic model building, it would be highly desirable to have accurate knowledge of the speed of response of the emission analyzers. To the best knowledge of the authors and their colleagues, this information is not available, and is essentially impossible to determine in a dynamometer test cell. There is anecdotal evidence to suggest that the time constant of the analyzers is slow in relation to the dynamics of the TWC. Indeed, when post-catalyst emissions have been dynamically recorded during the bag tests described in Section II-A, using instruments very similar to the Pierburgs available in the test cell, discrepancies on the order of twenty to thirty percent are common. This is partially attributed to the dynamic response of the instrumentation. According to the technical specifications of the HC and NO_x analyzers, the 90% rise time can be as much as 2 seconds, and its measurement error at each point can be up to ±1% of its current scale, regardless of the cur-

rent measurement. For example, when the measurement is at 20% of full scale, the relative measurement error can be as high as 5%.

Figures 7 and 8 compare post-catalyst measurements of HC and NO_x concentrations made with two different analyzers. One set of measurements is collected with the Pierburg emission analyzer, and the other set is taken with so-called *fast analyzers*. The fast analyzers are made by Horiba, model MEXA-1100FRC to measure NO_x and MEXA-1100FRF to measure HC. For a variety of practical reasons, these analyzers are not used for routine data collection.

Figures 9 and 10 show the TWC efficiency calculations based on the different measurements. Since only one set of fast analyzers was available, true fast efficiency calculations could not be performed. A rough approximation was used, though, calculated from the fast measurements of post-catalyst concentrations along with the slower pre-catalyst measurements. These plots show that, especially in the HC efficiency comparison, the dynamic response of the emission data set is probably poor.
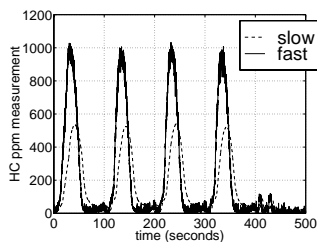

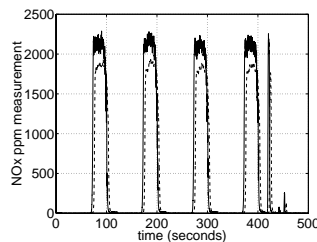Fig. 7. Slow and fast HC measurements.

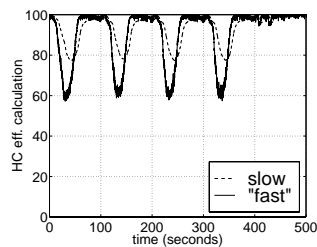Fig. 8. Slow and fast NO_x measurements.

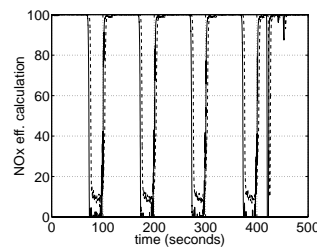

Fig. 9. Slow and "fast" HC efficiency calculations.

Fig. 10. Slow and "fast" NO_x efficiency calculations.

C. A/F measurement

Pre- and post-catalyst A/F were measured with a linear Exhaust Gas Oxygen (EGO) sensor, commonly called a UEGO sensor. Those used in this work are instrumentation grade, model MO-1000 sensors made by NTK at a cost of about $9000.00 each. These sensors are commonly modelled by a single 300-ms time constant. However, during extended excursions from stoichiometry, especially in the rich direction, additional dynamics may be present. Figure 6 (see also Fig. 16) shows a "bias" in the measured tailpipe A/F. It is unknown whether this is due to the sensor or to slow dynamics in the TWC, since the sensor itself operates on principles similar to those of the TWC.

The availability of measurements in a vehicle is subject to greater limitations than the laboratory environment. Instead of a linear sensor (UEGO), a vehicle will typically contain a switching HEGO sensor. The HEGO sensor does not provide a linear measurement of A/F but instead is a virtual switch [11], indicating whether the air-fuel mixture is rich or lean but not providing a good quantitative measurement. No on-board sensors for emissions are currently available.

IV. A Phenomenological TWC Model

A. Basic structure

The goal is to construct a simplified model which will predict conversion efficiencies under transient conditions. The structure of the proposed TWC model is shown in Fig. 11. The basic idea is to decompose the model into three parts: the standard steady state efficiency curves driven by tailpipe A/F, an oxygen storage mechanism to account for the modification of the A/F of the feedgas as it passes through the catalyst, and the thermodynamics of catalyst warm-up. The critical idea for representing the transient aspects of the TWC is that the only way for A/F to change while passing through the catalyst is for oxidation and/or reduction reactions to have occurred. Hence, the time constant of A/F changes may be taken as a crude indicator of the time constant of the reactions that take place in the catalyst. This is important because A/F is by far the fastest available measurement.
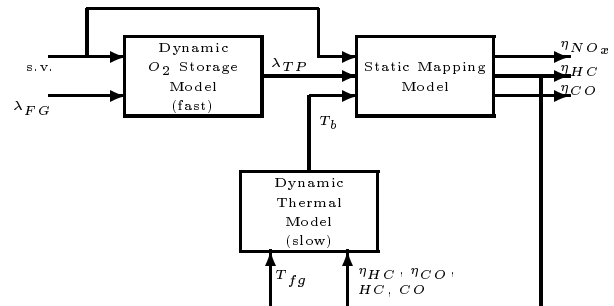

Fig. 11. Structure of the proposed TWC model.

In order to initially validate the proposed structure, equivalent tailpipe A/F was measured for a warmed-up catalyst and run through the measured static conversion efficiencies represented in Fig. 3. The results were then compared to measured conversion efficiencies. The agreement was good for NO_x and CO efficiency. The measured HC efficiency appeared to be a low-pass filtered version of the predicted conversion efficiency. After discussion with other engineers involved in emissions testing, and in light of Figs. 7 and 9, this was deemed to be primarily a measurement problem and not necessarily an invalidation of the model structure. Reference [4] discusses the fact that there may be other issues contributing to the mismatches between the test cell data and the model predictions.

In Subsections IV-B–IV-D, the oxygen storage, thermodynamic, and static conversion models are described. Sec-

tion V compares the model's performance with actual emissions data.

B. Oxygen storage sub-model

Let $0 \leq \Theta \leq 1$ be the fraction of oxygen storage sites occupied in the catalyst. The oxygen storage capacity is modeled as a limited integrator in the following way:

$$\dot{\Theta} = \begin{cases} \frac{1}{C} \times \rho(\lambda_{FG}, \Theta, MAF) \times 0.21 \times MAF \times \left(1 - \frac{1}{\lambda_{FG}}\right) \\ \qquad\qquad\qquad\qquad\qquad\qquad\qquad 0 \leq \Theta \leq 1 \\ 0 \\ \qquad\qquad\qquad\qquad\qquad\qquad\qquad \text{otherwise} \end{cases} \tag{10}$$

where
- $\dot{\Theta}$ represents $\frac{d\Theta}{dt}$;
- C represents the effective catalyst "capacity," or the volume of active sites for oxygen storage, expressed in terms of the mass of oxygen that can be stored in the catalyst;
- ρ describes the exchange of oxygen between the exhaust gas and the catalyst;
- λ denotes the relative air-fuel ratio, with stoichiometry at $\lambda = 1$ (the subscript FG refers to the feedgas);
- and MAF denotes the mass air flow rate, used to approximate the flow rate of the mixture entering the TWC.

The function ρ is modeled as

$$\rho(\lambda_{FG}, \Theta, MAF) = \begin{cases} \frac{1}{f_V(MAF)} \alpha_L f_L(\Theta) & \lambda_{FG} > 1 \\ \frac{1}{f_V(MAF)} \alpha_R f_R(\Theta) & \lambda_{FG} < 1 \end{cases} , \tag{11}$$

with $0 \leq f_L \leq 1$ representing the fraction of oxygen (combined or free) from the feedgas sticking to a site in the catalyst, and $0 \leq f_R \leq 1$ representing the fraction of oxygen being released from the catalyst and recombining with the feedgas. In (11), f_L and f_R vary with the fraction of occupied oxygen sites and potentially with the feedgas (or "space") velocity as well. In the model, f_L is assumed to be monotonically decreasing, with value one at $\Theta = 0$ and zero at $\Theta = 1$, and f_R is assumed to be monotonically increasing, with value zero at $\Theta = 0$ and one at $\Theta = 1$. Typical functions[2] f_L and f_R are shown in Figs. 12 and 13. The parameters α_L and α_R are included to represent the fact that the catalyst's storage and release rates of oxygen are different, with the release rate normally being higher than the storage rate.

The term $f_V(MAF)$ accounts for the effect of flow rate, or space velocity, on the storage capacity of the catalyst. It is represented by linear interpolation between the entries from Table II. This effect is only active near idle conditions.

The quantity $0.21 \times MAF \times (1 - \frac{1}{\lambda_{FG}})$, which can be rearranged to $0.21 \times MAF \times \frac{\Delta \lambda_{FG}}{\lambda_{FG}}$, represents the differential total mass of oxygen (combined or free) in the feedgas with respect to stoichiometry. When multiplied by ρ, it gives the

[2]Recall the plateau in the tailpipe A/F that occurs as the feedgas is switched from lean to rich. To capture this in the model, it is necessary that f_R be equal or nearly equal to one for some nontrivial range of Θ near zero. Similarly, it is necessary that f_L be equal or nearly equal to one for some nontrivial range of Θ near one.
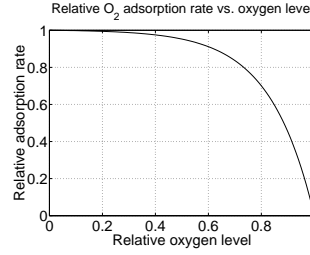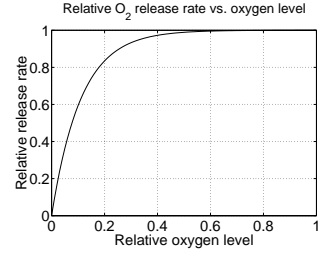

Fig. 12. Typical function f_L.

Fig. 13. Typical function f_R.

MAF (lb/hr)	$f_V(MAF)$
50	25
80	80
240	240

TABLE II
$f_V(MAF)$

mass of oxygen that is deposited in (or released from) the catalyst. By conservation of mass, the resulting equivalent tailpipe A/F can be directly computed by the following:

$$\lambda_{TP} = \lambda_{FG} - \rho(\lambda_{FG}, \Theta, MAF) \times \frac{MAF}{S} \times \left(1 - \frac{1}{\lambda_{FG}}\right), \tag{12}$$

where S is the stoichiometric value (near 14.5 for most blends of gasoline).

For the oxygen storage submodel, the effects of feedgas and catalyst temperature are currently not included. The block diagram representation of the oxygen storage submodel is shown in Fig. 14.
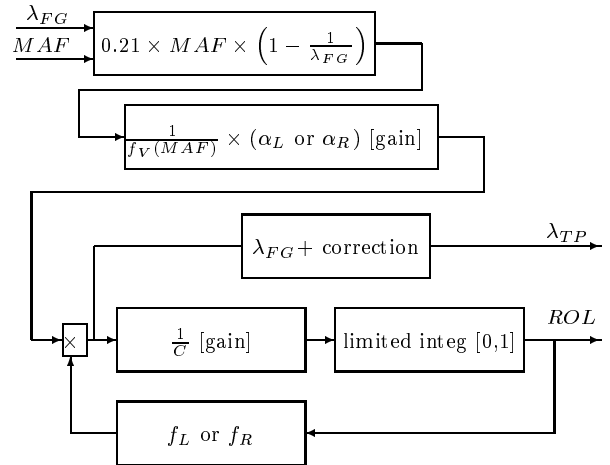

Fig. 14. Structure of the oxygen storage submodel.

Reference [10] contains an oxygen storage model that is similar to (10), but it does not include the nonlinear storage and release terms proposed in (11) (or the correction for space velocity). As a consequence, the model of [10] cannot capture the oxygen storage plateau that is evident in Figs. 5, 6, 16, and 19.

In order to automate the tuning process of the oxygen storage submodel against data, an optimization routine was used to adjust model parameters in a systematic fashion. The particular cost function was a sum of the mean square errors to the five input signals shown in Fig. 15. The square waves provided a representation of the step response characteristic, while the triangle waves provided a ramp response. Since there were significant differences in these responses, the clipped triangle waves were used to obtain responses to sharper ramps, closer to steps.

The accuracy of the model in predicting tailpipe A/F for a warmed-up catalyst is shown in Fig. 16.
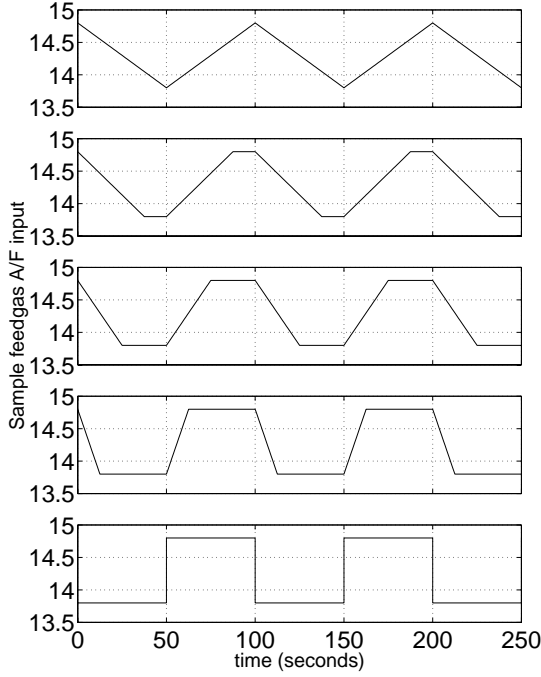

Fig. 15. Sample feedgas A/F excitation signals.

Fig. 16. Model fit for warmed-up catalyst.
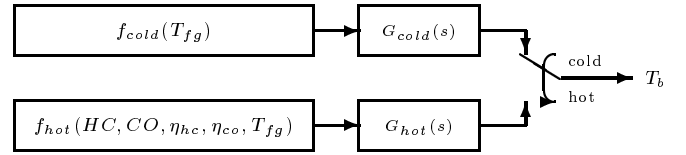
Fig. 17. Block diagram of brick temperature model.

C. Heat transfer sub-model

In order to adequately model the conversion efficiencies of a TWC in an arbitrary drive cycle, catalyst temperature must be taken into account. Especially during cold start, catalyst temperature plays a key role in determining the light-off time. Before light-off, catalyst temperature changes are due to thermal energy absorption from the feedgas. After light-off, these temperature changes are primarily due to a combination of thermal and chemical processes. This difference in model behavior is depicted in Fig. 17, and is represented by

$$\dot{T_b} = \begin{cases} \frac{1}{\tau_1}\left[-T_b + f_{cold}(T_{fg})\right] & T_b < \text{threshold} \\ \frac{1}{\tau_2}\left[-T_b + f_{hot}(HC, CO, \eta_{hc}, \eta_{co}, T_{fg})\right] & T_b > \text{threshold} \end{cases}$$

$$(13)$$

where T_b represents the brick temperature; τ_1 and τ_2 are the first order time constants; T_{fg} represents the temperature of the feedgas; HC and CO represent feedgas emission levels of hydrocarbons and carbon monoxide, respectively;
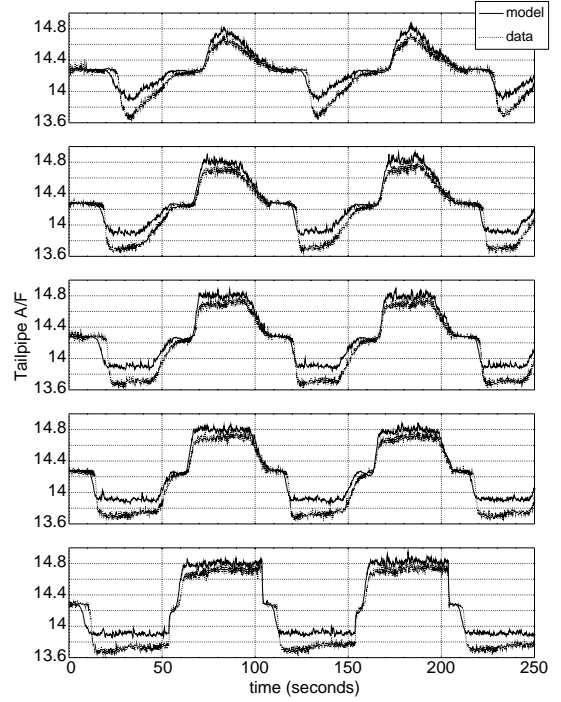
and η_{hc} and η_{co} represent the efficiencies of the TWC in oxidizing HC and CO. The nonlinear functions $f_{cold}(T_{fg})$ and $f_{hot}(HC, CO, \eta_{hc}, \eta_{co}, T_{fg})$ and the two time constants are determined by regression against measured data.

The cold start functions from (13) and Fig. 17 are as follows:

$$f_{cold}(T_{fg}) = 1.5 T_{fg} \qquad (14)$$

$$G_{cold}(s) = \frac{1}{23.9s + 1} \qquad (15)$$

The corresponding warmed-up functions are as follows:

$$f_{hot}(HC, CO, \eta_{hc}, \eta_{co}, T_{fg}) =$$
$$-680.019 + 13.9492 \cdot \alpha_T + 2.18290 \cdot T_{fg}$$
$$-0.128667 \cdot \alpha_T^2 - 0.00186859 \cdot T_{fg}^2$$
$$+0.0132708 \cdot \alpha_T \cdot T_{fg} \qquad (16)$$

$$G_{hot}(s) = \frac{1}{8.9s + 1} \qquad (17)$$

where α_T is the equivalent temperature arising from the heat generated by the chemical process inside the TWC after light-off, calculated as follows:

$$\alpha_T = \frac{153.5 \cdot \eta_{hc} \cdot HC + 67.72 \cdot \eta_{co} \cdot CO}{153.5 \cdot HC + 67.72 \cdot CO} \qquad (18)$$

and the temperature is expressed in degrees Fahrenheit. The threshold for switching from the cold to the hot dynamics is 650°F.

Model results are compared with measurements from Bag 1 of the FTP cycle in Fig. 18 and show good agreement.
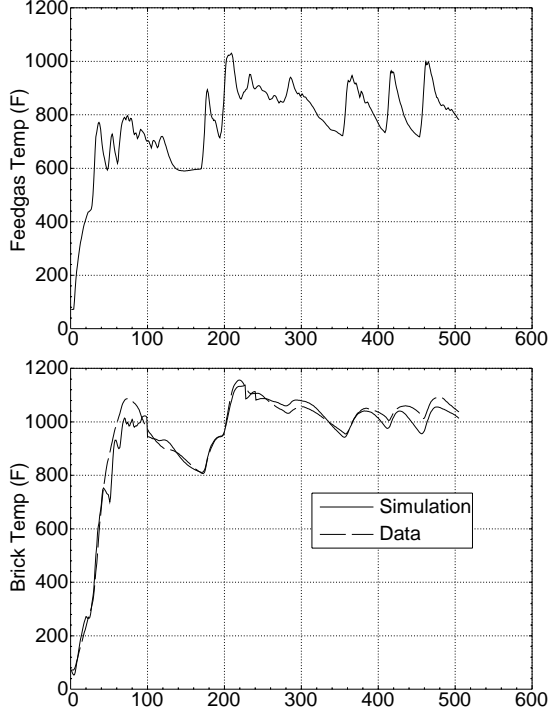

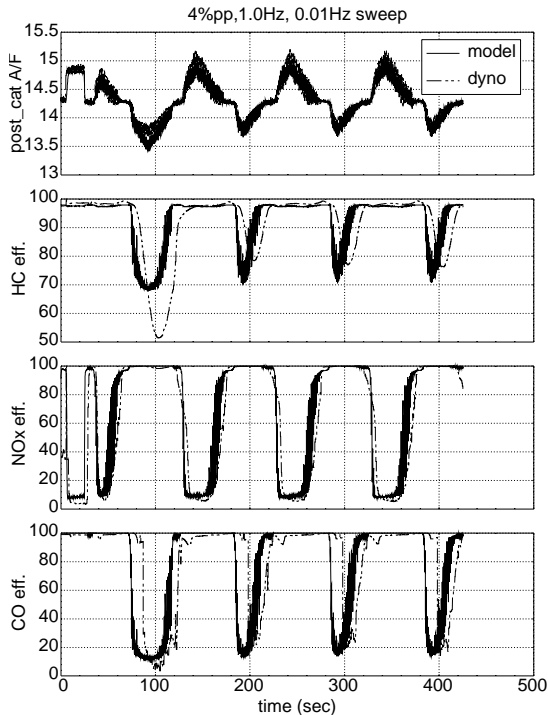Fig. 18. Feedgas and brick temperatures vs. time in Bag 1.

Fig. 19. Validation data for warm TWC model.

D. Static conversion curves

The static behavior of a TWC is characterized by the conversion efficiencies of HC, CO, and NO_x as functions of the tailpipe air-fuel ratio. These functions for the specific TWC used in this paper are plotted in Fig. 3 for a constant brick temperature. There is a narrow window of air-fuel ratio around the stoichiometric point within which the high conversion efficiencies of all three pollutants can be achieved for a typical three-way catalyst. However, the inlet temperature, which is measured at about half an inch from the face of the first brick of the TWC, also affects the conversion efficiency, and the effects are significant enough to make a difference in the subsequent control design and optimization analysis [5].

Tests were conducted to map the catalyst conversion efficiency for different air-fuel ratio and brick temperature setpoints. The data used in this part of the modeling work were collected under steady state, warmed-up engine conditions. For each engine speed/load point, the spark timing was adjusted to meet the desired temperature before a ± 1.0 air-fuel ratio sweep was applied. The dynamometer test data show that the HC, CO, and NO_x conversion efficiencies are sensitive to the variations in temperature.

The nonlinear functions representing the static efficiency curves are derived by regressing the dynamometer test data with respect to normalized air-fuel ratio and brick temperature. The HC conversion efficiency is then corrected by a linear function of the mass air flow rate, which accounts for the effect of space velocity on the catalyst performance. In order to achieve better numerical results during the regression, the temperature and air-fuel ratio variables are first normalized as follows:

$$\hat{T}_b = \frac{T_b - 496}{1188} \tag{19}$$

$$r_H = \frac{r_{pc} - r_{st} + 3.885}{7.43} - 0.0339\hat{T}_b + 0.0058$$

$$r_C = \frac{r_{pc} - r_{st} + 3.68}{7.43} - 0.0086 \tag{20}$$

$$r_N = \frac{r_{pc} - r_{st} + 3.6}{7.43}$$

where $\hat{T}_b, r_H, r_C, r_N$ are normalized variables for the brick temperature, HC specific, CO specific, and NO_x specific air-fuel ratio respectively. Then the static catalyst performance is described by the following conversion efficiency equations for the three pollutants:

$$\eta_H = 1.0021 \left(\gamma_H + \frac{(0.998 - \gamma_H)r_H^{14}(-0.1r_H + 1.061)}{p_H(r_H)} \right)$$
$$+ (-0.0292\dot{m}_a - 0.003075) \tag{21}$$

$$\eta_C = 1.0229 \left(\gamma_{C1} + \frac{0.9886 r_C^{16} \gamma_{C2}}{p_C(r_C)} \right) \tag{22}$$

$$\eta_N = \frac{1}{1 + e^{-\frac{r_N - 0.49304}{0.00576}}} \left(-1.5425 + \frac{7.32456}{1 + e^{-\frac{\hat{T}_b + 2.95654}{1.47271}}} \right)$$
$$- \frac{0.05074}{1 + e^{-\frac{\hat{T}_b + 2.95654}{1.47271}}} + 1.00475 \tag{23}$$

where $\gamma_H, \gamma_{C1}, \gamma_{C2}$ reflect the temperature effects on HC and CO conversion efficiency, empirically defined as:

$$\gamma_H = 0.3654\hat{T}_b + 0.5555$$
$$\gamma_{C1} = 0.4752\hat{T}_b - 0.0616$$
$$\gamma_{C2} = 0.0706\hat{T}_b^2 - 0.6981\hat{T}_b + 1.2058$$
$$- r_C(0.1411\hat{T}_b^2 - 0.4459\hat{T}_b + 0.2924), \quad (24)$$

where p_H and p_C are Chebyshev polynomials of 14th and 16th order, respectively, whose coefficients are defined in Table III.

Function Term	HC Efficiency parameter	CO Efficiency parameter
const.	0.014558	0.0020713
x^2	-0.2038	-0.034509
x^4	1.12097	0.23355
x^6	-3.0571	-0.82298
x^8	4.2791	1.6064
x^{10}	-2.8540	-1.7026
x^{12}	0.7137	0.88634
x^{14}	0.399	-0.1759
x^{16}	1	1

TABLE III

Catalyst Static Efficiency Function Parameters for HC and CO

V. Overall Model Evaluation

Figure 19 shows a comparison between test data and simulation data from the dynamic catalyst model of Section IV. At this warm condition, the feedgas A/F is the only input to the model, and the comparison is shown to be quite favorable for tailpipe A/F as well as NO_x and CO conversion efficiencies. However, the model seems to underestimate the HC conversion efficiencies during the rich portions of the test. At the time of writing, it is unknown how much of this error is due to modeling errors and how much of it is due to the dynamics of the emission analyzers.

The entire TWC model can be used in combination with either an engine model or actual feedgas emission data to predict tailpipe emissions [5]. Based on feedgas A/F, a tailpipe A/F estimate is calculated in the oxygen storage submodel. Then, temperature corrections are applied to the static efficiency curves. The tailpipe A/F estimate is then input to the corrected static efficiency curves, yielding TWC efficiency numbers for HC, NO_x, and CO. Given feedgas emission levels of each of these components, tailpipe emissions can then be estimated.

In order to test the predictive capability of the model, FTP emissions data were obtained from a different TWC of the same type as modelled in Section IV, mounted on a vehicle. A comparison to available FTP cycle data is shown in Table IV. The simulation data are based on feedgas A/F and emissions data that were collected from a vehicle running the FTP cycle. The emission analyzers were similar

		Simulation	Bag Data	% Error
Bag 1	HC	2.85	2.33	22.3%
	CO	16.2	19.1	-15.2%
	NO_x	0.762	1.03	-26.0%
Bag 2	HC	0.0294	0.0289	1.73%
	CO	0.234	0.232	0.86%
	NO_x	0.218	0.279	-21.9%
Bag 3	HC	0.276	0.200	38.0%
	CO	0.365	0.283	29.0%
	NO_x	0.580	0.679	-14.6%

TABLE IV

Comparison of mass emissions (in grams) between simulation and bag data.

to those in the dynamometer test cell. The table shows accumulated tailpipe mass emissions from each bag of the cycle along with the model estimate of these values. The differences in the results from Bags 1 and 3 highlight the need for further work on the model's performance under startup conditions. However, the Bag 2 results, especially for HC and CO, are encouraging, despite the need for improvement in tailpipe NO_x estimation.

VI. Conclusion and Remaining Issues

A simplified dynamic model of a three-way catalytic converter has been developed and validated against dynamic A/F and emissions data. The model captures the funamental transient oxygen storage and thermal characteristics of the TWC, plus the standard steady state conversion efficiencies.

The preliminary validation of the model against data seems quite favorable. There are, however, many issues that remain to be investigated. For example, there are some indications that there is more going on in the TWC than just the oxygen storage, especially for rich A/F, where slow dynamics appear. When A/F is held rich for several minutes at the end of a test, a much slower "settling" of A/F to a steady state value is seen. In addition, more startup data (cold and hot start) needs to be collected in order to expand the capability of the thermal model.

Finally, the TWC converter is clearly a distributed device. A single lumped element model has been presented in this paper. The oxygen storage model in particular can be cascaded with itself in order to better approximate the distributed nature of the catalyst. A cascaded model may also be useful for representing TWC's that are composed of multiple bricks of different catalytic material. Each brick could then be represented by an individual oxygen storage block.
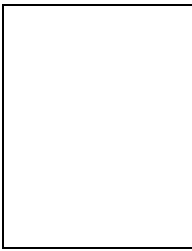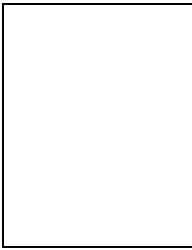
REFERENCES

[1] A. Stefanopoulou, *Modeling and Control of Advanced Technology Engines*, Ph.D. thesis, University of Michigan, Feb. 1996.

[2] C. N. Montreuil, S. C. Williams, and A. Adamczyk, "Modeling current generation catalytic converters: Laboratory experiments and kinetic parameter optimization-steady state kinetics," SAE paper 920096, Society of Automotive Engineers, 1992.

[3] K. N. Pattas, A. M. Stamatelos, P. K. Pistikopoulos, G. C. Koltsakis, P. A. Konstandinidis, E. Volpi, and E. Leveroni, "Transient modeling of 3-way catalytic converters," SAE paper 940934, Society of Automotive Engineers, 1994.

[4] H. J. Germann, C. H. Onder, and H. P. Geering, "Fast gas concentration measurements for model validation of catalytic converters," SAE paper 950477, Society of Automotive Engineers, 1995.

[5] J. Sun and N. Sivashankar, "An application of optimization methods to the automotive emissions control problem," in *Proceedings of the 1997 American Controls Conference*, June 1997.

[6] P. R. Crossley and J. A. Cook, "A nonlinear model for drivetrain system development," in *IEE Conference Publication 332*, Edinburgh, U.K., Mar. 1991, vol. 2, pp. 921–925.

[7] John B. Heywood, *Internal Combustion Engine Fundamentals*, McGraw-Hill, Inc., 1988.

[8] Automotive Information Center, "Catalytic converters," World Wide Web, URL: http://www.autosite.com/garage/subsys/bacataly.asp.

[9] Environmental Protection Agency, "Automobile emissions: an overview," Aug. 1994, World Wide Web, URL: http://www.epa.gov/OMSWWW/05-autos.htm.

[10] E. Shafai, C. Roduner, and H. P. Geering, "Indirect adaptive control of a three-way catalyst," SAE paper 961038, 1996 SAE International Congress, Detroit, MI, February 1996, included in *SAE Special Publication SP-1149, Electronic Engine Controls*.

[11] J. T. Woestman and E. M. Logothetis, "Controlling automotive emissions," *The Industrial Physicist*, vol. 1, no. 2, pp. 20–24, Dec. 1995.

[12] E. P. Brandt, Yanying Wang, and J. W. Grizzle, "A simplified three-way catalyst model for use in on-board SI engine control and diagnostics," in *Proceedings of the ASME Dynamic Systems and Control Division*, G. Rizzoni, Ed. American Society of Mechanical Engineers, Nov. 1997, vol. 61, pp. 653–659, 1997 ASME International Congress and Exposition, Sixth ASME Symposium on Advanced Automotive Technologies.
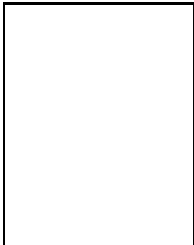
Yanying Wang was born in GuangXi, China. She received the B.S. and M.S. degrees from Tsinghua University, Beijing, China, in 1982 and 1985, respectively. She received the Ph.D. degree in Mechanical Engineering from Michigan State University in 1992. From 1992 to 1995, she worked on site at Ford Motor Company as a mechanical engineer for couple of industrial firms. She joined Scientific Research Laboratory of Ford Motor Company, Dearborn, Michigan, in 1995. She has been working on SI engine combustion simulation, vehicle suspension system modeling with Bond Graph technique, and modeling and control of powertrain and emission systems.

Jessy W. Grizzle received the Ph.D. in electrical engineering from The University of Texas at Austin in 1983. Since September 1987, he has been with The University of Michigan, Ann Arbor, where he is a Professor of Electrical Engineering and Computer Science. He is a past Associate Editor of the Transactions on Automatic Control and Systems & Control Letters, served as Publications Chairman for the 1989 CDC, and in 1997 was elected to the Control Systems Society's Board of Governors. Dr. Grizzle's major research interests lie in the field of control systems. Since his doctoral work, he has investigated theoretical questions in nonlinear systems, where he has concentrated on discrete-time problems and observer design. He has been a consultant in the automotive industry since 1986, where he jointly holds several patents dealing with emissions reduction through improved control system design. In 1992, along with K.L. Dobbins and J.A. Cook of Ford Motor Company, he received the Paper of the Year Award from the IEEE Vehicular Technology Society. Since 1991 he has been working with an interdisciplinary team of researchers at the University of Michigan on applying systems and control techniques to improve the operation of plasma-based microelectronics manufacturing equipment. Dr. Grizzle was a NATO Postdoctoral Fellow from January to December 1984; he received a Presidential Young Investigator Award in 1987, the University of Michigan's Henry Russell Award for outstanding research in 1993, a College of Engineering Teaching Award, also in 1993, and was made a Fellow of the IEEE in 1997.

Erich P. Brandt is currently working toward a Ph.D. from the Electrical Engineering and Computer Science Department at the University of Michigan in Ann Arbor. He received his B.S. in Computer and Electrical Engineering and M.S. in Electrical Engineering from Purdue University, West Lafayette, Indiana, in December 1992 and May 1994, respectively. Since 1990, he has worked in various departments as a summer intern and, later, a supplemental employee at Ford Motor Company. He is currently working in the Powertrain Control Systems Department at the Ford Research Laboratory, where he has been employed on a part time basis since 1994.